GPS and UWB for indoor navigation

Guttorm Ringstad Opshaug and Per Enge

Department of Aeronautics and Astronautics, Stanford University

Abstract

A multitude of applications would benefit from precise indoor navigation. Anywhere from automating storage in warehouses to tracking firemen in hazardous environments would make such an endeavor worthwhile.

Some server-based GPS systems, like SnapTrack, already claim some navigation capabilities indoors. However, such systems are in general accurate to within a few tens of meters. Furthermore, pseudolites have been deployed for indoor use. Although some experimental setups show decent navigation performance, there is a question of whether GPS has a "good enough" signal structure for such applications in the first place.

Spread spectrum pseudoranging is susceptible to multipath that is less than one chip width away from a direct path ray. In the case of GPS C/A-code, the chip length is about 300 m. Obviously, most indoor signal reflection delays would be significantly shorter than that distance.

Ultra-WideBand (UWB) technology is built around transmitting short discrete pulses instead of continuously modulating a code onto a carrier signal. Such pulses typically last only 1-2 ns, and one can distinguish pulses that are more than 1-2 ft apart. Thus, making UWB systems robust to multipath delays of more than one pulse width.

We measured the impulse response of the RF channel at the Stanford University LAAS Laboratory. This paper quantifies that multipath channel in terms of average delay and delay spread. We found several cases where multipath components were stronger in magnitude than the direct signal. Whereas such an environment would bias pseudorange measurements of GPS C/A-code, a properly designed UWB system could resolve most multipath and accuracy would degrade more gracefully than for GPS.

Introduction

Spread spectrum signals, such as the GPS C/A-code, are robust against many forms of interference. The process of correlation strongly suppresses the effects of one C/A-code on another. Similarly, the auto-correlation function of a C/A-code has one peak that is more than 20 dB stronger than any sub-peak.

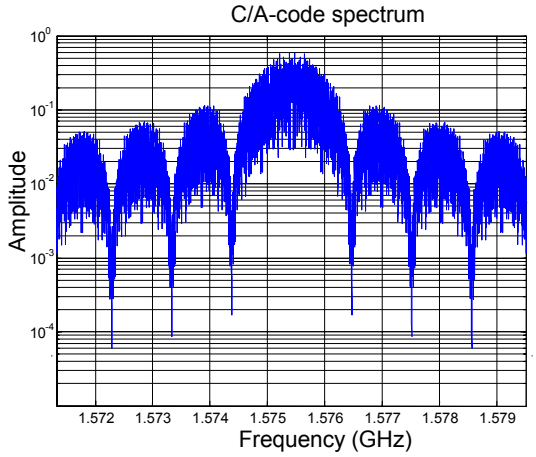

Figure 1: C/A-code spectrum

However, multipath components that occur within the correlator peak may well result in code phase errors. Several approaches are used to reduce the effects of multipath. Multipath limiting antennas (MLAs) are used in some stationary applications [1] and such antennas suppress low elevation signal paths. Most GPS receivers use narrow correlator techniques [2], i.e. they track high up on the correlator peak. Such narrow correlators reduce absolute values of multipath pseudorange errors.

Ultra-WideBand (UWB) technology emerged during the 1960s in an attempt to characterize microwave n-ports through their impulse response [3]. Such measurements were done by sending very short pulses into RF devices and looking at their transmissions and reflections at all ports. The first UWB patent was awarded Sperry in 1973 [4]. This technology started to come of age in land mine detection [5] and foliage penetrating radars [6] in the late 90's. Several companies and universities are working on communications applications (e.g. MSSI and USC's Ultra Lab), and even navigation applications (Æther Wire & Location, Inc.), for UWB technology.

UWB is somewhat loosely defined as signals with frequency content that fulfills the following equation for fractional bandwidth [7]:

$$BW_{fractional} = 2 \cdot \frac{(f_{hi} - f_{low})}{(f_{hi} + f_{low})} > 0.25 \qquad \text{Eq.1}$$

The equation does not include any carrier frequency, but rather uses limits for higher, f_{hi}, and lower, f_{low}, signal frequency content.

We further constrain UWB to be pulsed signals. In general such pulses last 1-2 ns, and have bandwidths of several GHz, i.e. about 1000-fold that of the GPS C/A-code main lobe. The two figures below show typical time and frequency domain characteristics of UWB signals (Courtesy of Ming Luo and Dennis Akos).

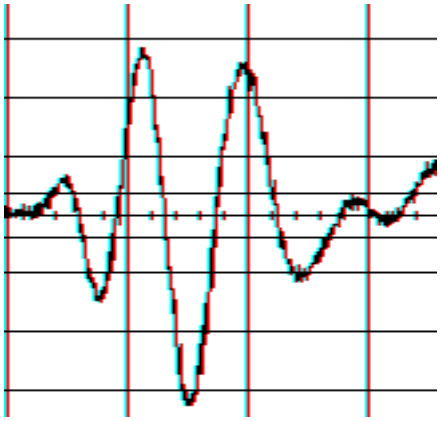

Figure 2: Typical UWB pulse

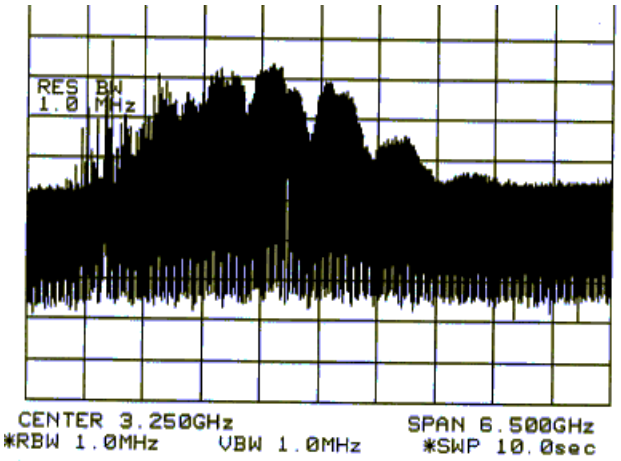

Figure 3: Typical UWB spectrum

Obviously, such signals radiate inside the frequency bands of other services, but the claim is that UWB power density can be made so low that it won't adversely affect other radio systems. As of yet, this is an unresolved issue with the FCC, although it is unlikely that UWB will be deployed un-attenuated in frequency bands below 3 GHz.

Even though there are a few technical and political issues involved with UWB technology, it does show great promise for signal penetration in buildings and has an almost infinite spectral diversity. Since UWB pulses last about 1-2 ns, one can distinguish pulses that are more than 1-2 ft apart. In this way, multipath components outside one pulse width can be eliminated and only ultra-in-close reflections affect ranging.

Multipath envelope simulations

To strengthen our beliefs regarding multipath errors for GPS and UWB systems, we simulated the following single reflection scenario: Keeping both a transmit and a receive antenna stationary, we gradually move a reflector away from the receive antenna. The figure below shows a block diagram of our model.

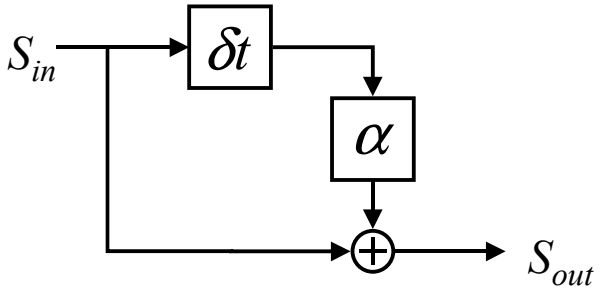

Figure 4: Single reflection multipath model

A worst case multipath envelope for GPS is generated when the reflection is either fully added or fully subtracted from the direct signal on the carrier phase level. Thus, we used the following equation for the total received signal:

$$S_{out}(t) = S_{in}(t) + \alpha \cdot S_{in}(t - \delta t) \qquad \text{Eq. 2}$$

In the simulations we used a reflection coefficient, α, of ±0.5, and we swept the delay, *dt*, from 0 m to 300m. This should be considered severe multipath. We correlated the total signal, $\boldsymbol{S}_{out}$, with a perfect C/A-code. Finally, we straddled the correlation peak with two correlators 0.1 chip-width apart. The figure below shows the multipath envelope for the given reflection coefficient and correlator spacing.

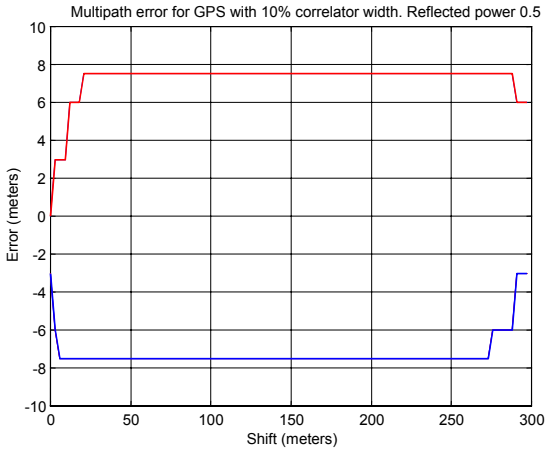

Figure 5: GPS multipath envelope

A similar simulation was conducted using real measurements of a UWB sounding pulse. The UWB pulse lasted about 1 ns, and we again invoked the concept of correlation to find the multipath envelope. The two

correlators were spaced 0.1 pulse-width apart, i.e. 100 ps. Figure 6 shows the UWB multipath envelope.

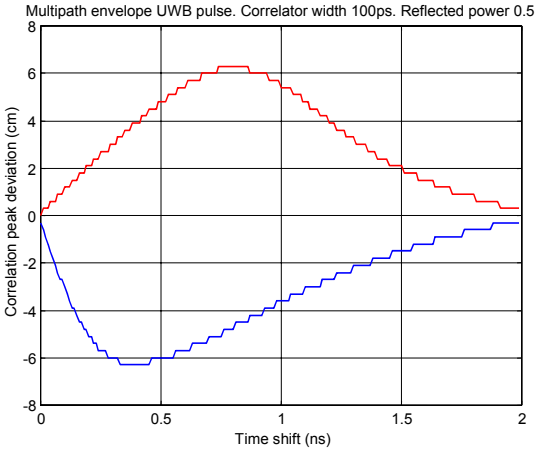

Figure 6: UWB multipath envelope

Whereas our simulations predict a worst case pseudorange error of ±6 cm in the UWB case, the corresponding GPS error is nearly ±8 meters.

Background

The field of digital communications deal with bit-error rates and bit-energy to noise ratios. Multipath may lead to inter-symbol interference (ISI) as well cause fading by destructively subtracting from a direct path signal. However, multipath is used constructively in Rake receivers [8] to capture more energy to better determine correct bit values.

Whereas communication systems require signals to carry enough energy to a receiver, GPS-like navigation systems also require time of transmission and time of arrival information. Absolute delays between transmitters and a receiver must be determined in order to calculate user position. Thus, a multipath channel may adversely affect positioning availability through signal fluctuations (fading), as well as accuracy through biasing pseudorange measurements.

Channel modeling

The environment that a signal passes through from a transmitter to a receiver is referred to as the channel. Mobile Cellular Communications provide ample theory and measurement techniques for modeling signal propagation [9]. Signal channels are frequently described using the following parameters:

Average delay

$$\bar{\tau} = \frac{\int_{-\infty}^{\infty} t \cdot P(t)dt}{\int_{-\infty}^{\infty} P(t)dt} \qquad \text{Eq. 3}$$

Delay spread

$$\sigma_{delay} = \sqrt{\frac{\int_{-\infty}^{\infty} (t-\bar{\tau})^2 \cdot P(t)dt}{\int_{-\infty}^{\infty} P(t)dt}} \qquad \text{Eq. 4}$$

Doppler spread

$$\sigma_{Doppler} = \sqrt{\frac{\int_{-\infty}^{\infty} (f-f_0)^2 \cdot P(f)df}{\int_{-\infty}^{\infty} P(f)df}} \qquad \text{Eq. 5}$$

Average delay describes mean travel time of a signal from a transmitter to a receiver. Delay spread is a metric of how much that signal is diluted in time. Doppler spread tells us how signal energy smears out in frequency in situations where the environment and/or the transmit/receive antennas move. All measurements in this paper were conducted with both antennas and environment in static configurations, so Doppler spread is zero. Whereas average delay is analogous to the statistical parameter of mean, delay spread and Doppler spread compares to standard deviation (Power density function, *P(t)* or *P(f)*, vs. probability density function).

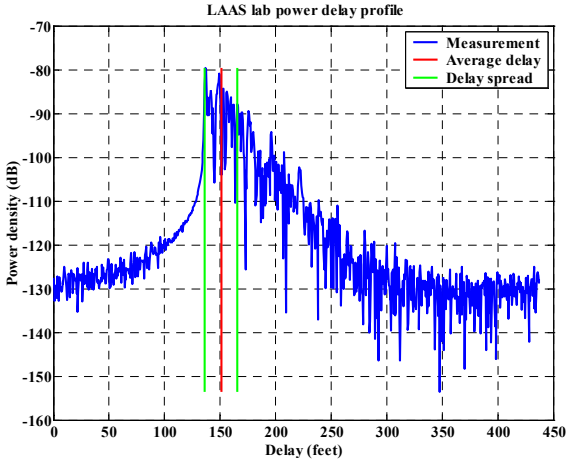

Figure 7: Sample impulse response w/ average delay and delay spread.

Rms. values for several point-measurements of the above parameters can be taken to describe the propagation environment over a larger area.

Measurement setup

Three main techniques exist for measuring radio-channels: sounding pulses, S-parameter measurements and frequency sweeping correlators. We had equipment readily available for the two first approaches, and we tested both techniques.

UWB sounding pulse

We connected a Hyperlabs HL9200 UWB pulser to a Tektronix 2021 Arbitrary Waveform Generator (AWG). The output of the pulser was connected to a UWB antenna through a JCA UWB amplifier. On the receiving end we used similar antennas and amplifiers, but in opposite order. The RF front-end output was then hooked up to an Agilent 86100a fast sampling oscilloscope with an Agilent 54754a TDR/TDT module. The pulser was triggered from the AWG, which also provided a synchronization pulse to the oscilloscope.

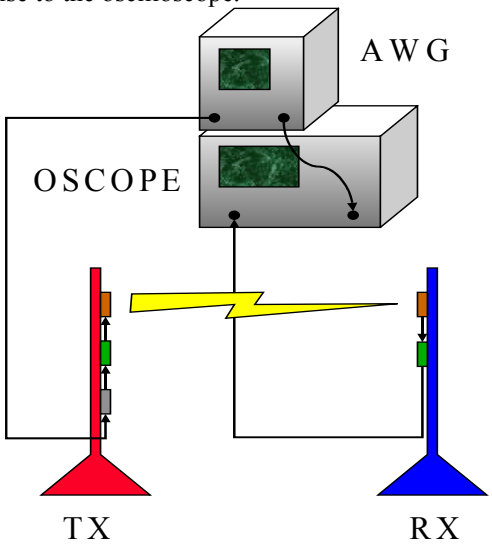

Figure 8: Sounding pulse test setup

The receive antenna was mounted 58 inches off the ground on a blue plastic pipe in a tripod stand. The receive setup was placed in a stationary location in the middle of the Stanford LAAS laboratory. A similar stand with a red plastic pipe was used for the transmit setup, and it was taken to 97 different measurement locations around the lab.

Finally, we surveyed locations of all significant metallic objects in the building. Figure 9 at the bottom of the page shows all measurement points and all metallic structures.

Figure 10 depicts a sample UWB sounding pulse measurement.

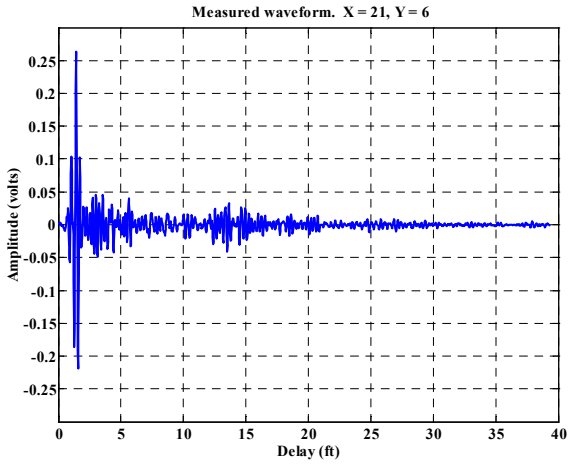

Figure 10: Sounding pulse measurement

S-parameter measurements

We first connected an HP 85046a S-parameter test set to an HP 4396a Network/Spectrum analyzer. The same pair of UWB antennas as before were connected to the S-parameter test set through long coax cables. See the figure below.

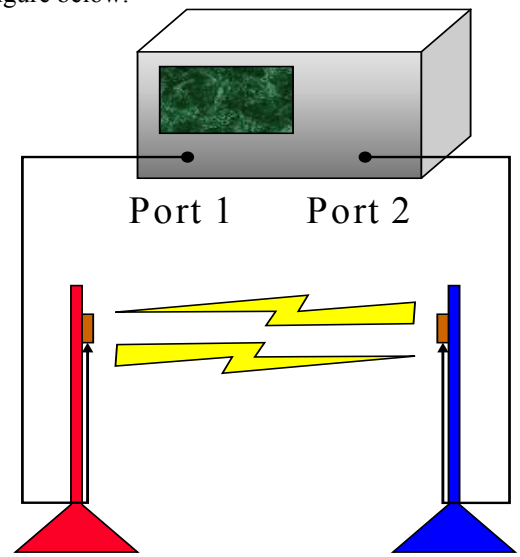

Figure 11: S-parameter test setup

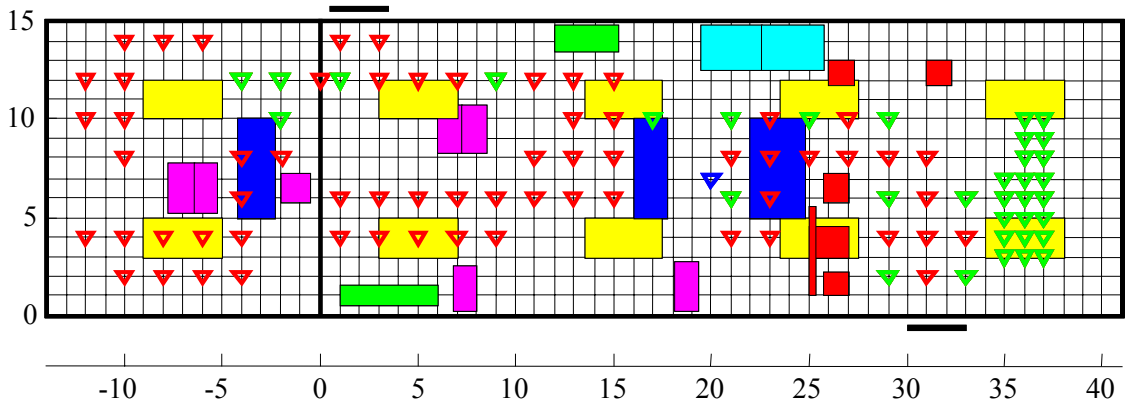

Figure 9: Measurement points and metallic objects. S-parameter: green UWB: red and green

After calibrating the coax cables, we placed the blue antenna stationary in the same location as above. The red antenna was then taken around to a subset of 35 different locations in the building (equipment failure prevented us from probing all 97 previous locations).

At each measurement point, frequency was swept between 1 MHz and 1.8 GHz in 801 steps. We found the impulse response from transmit to receive antennas by taking the inverse fast-fourier transform (IFFT) of the measured frequency response. Figure 12 shows the fundamental S-parameter measurement at location (21,6).

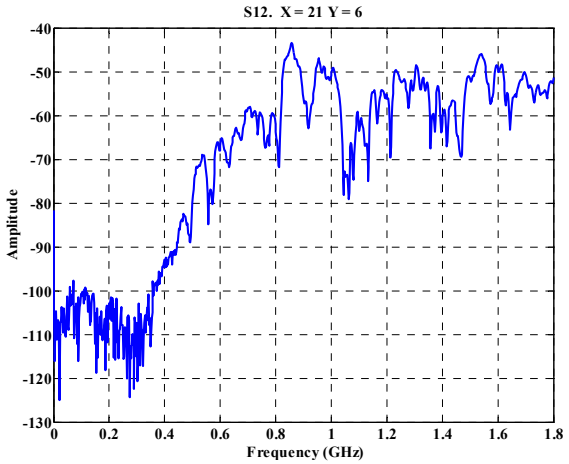

Figure 12: S-parameter measurement

Truth system

We used a tape measure to find the 58-inch UWB antenna heights. Both antennas were outfitted with plumbs so we could correct for the slightly uneven floor in the building. Noting that floor tiles in the LAAS lab are exactly 1 ft by 1 ft provided our horizontal position reference.

Channel modeling results

Average delays and delay spreads for both the sounding pulse and for the S-parameter measurements are plotted in Figures 13 and 14 respectively. Note that the S-parameter trials in general show greater average delay and delay spread than the sounding pulse ones.

There is a general increase in delay spread for distances beyond 20 ft. This may well be due to the wall located 20 ft from the receiver antenna.

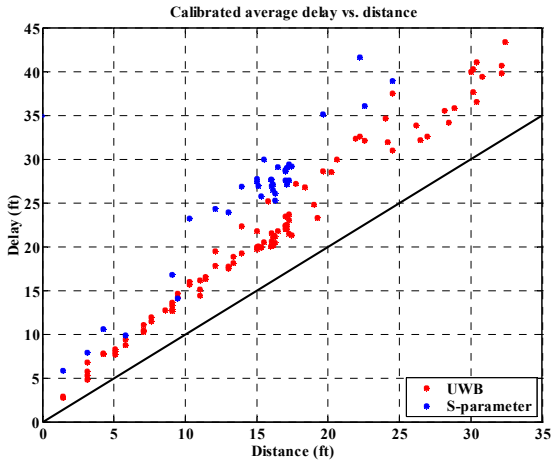

Figure 13: Average delay

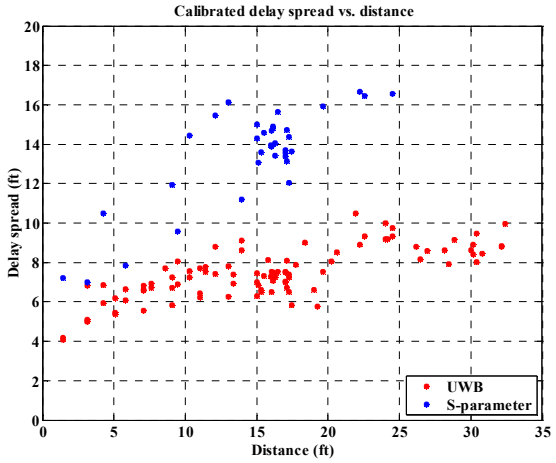

Figure 14: Delay spread

The next figure shows calibrated range errors from measurements of the strongest signal peak location.

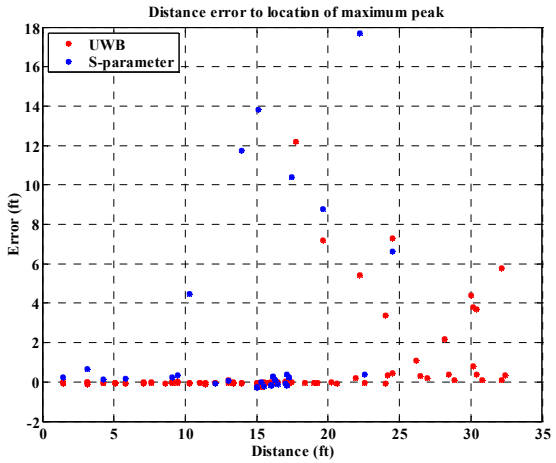

Figure 15: Strongest peak errors

The farther between the two antennas the greater the frequency of errors.

Total received power is plotted on the figure below.

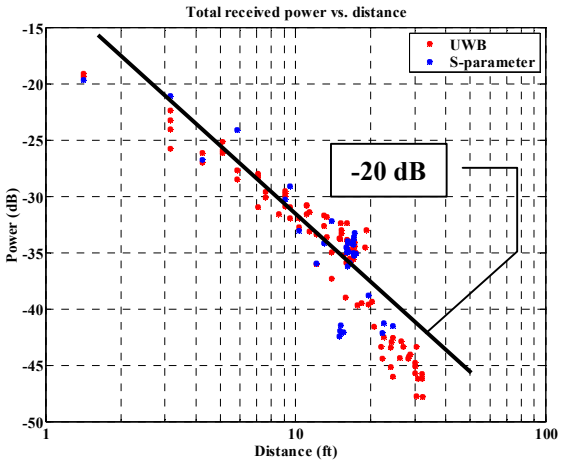

Figure 16: Total received power.

It is interesting to note that the general trend of the above plot is not $1/d^2$ (free space), but rather closer to $1/d^{1.5}$. This may well be due to the number of multipath components that add to the total power measurement. There is also a significant dip in the measurements around 20 ft. Again we attribute that effect to the building wall.

Conclusion

At short transmit/receive distances we find the direct signal to be significantly stronger than any multipath. As we move the transmitter farther away from the receiver, the direct signal becomes more equal in magnitude with multipath. At distances beyond 10 ft in the S-parameter measurements, and 17 ft in the UWB sounding pulse measurements, we find several cases where the arrival of the strongest signal component does not coincide with the first signal arrival. A GPS receiver would track the strongest signal, which would bias pseudorange measurements accordingly. However, the "early" multipath may alleviate some of those errors.

Average delay diverges linearly from the line of true distance. Delay spread also increases with distance, but seems to converge towards a constant value. Both measurement metrics indicate that signal energy is distributed over greater time intervals as distance grows.

Close to the transmitter future studies may find that the received power follows a Ricean probability distribution (one strong component and many small random ones). At greater distances, there may be several equally strong signal components, and the received power may better match a Rayleigh probability distribution (many equally strong random components). Such information can be used to generate availability and range charts for indoor GPS systems.

By measuring amplitude and arrival time of various signals in a multipath channel, one can model the corresponding pseudorange errors in a GPS receiver. In theory one could calibrate out those errors, but that would require a rather unrealistic stationary signal environment.

UWB technology has potential for avoiding ranging accuracy degradation for all but ultra-in-close multipath. Previous studies suggest UWB systems to be void of deep fades [10]. Thus, system range and availability tables might be calculated more deterministically even in multipath rich environments.

There is of course great potential for integrating UWB with GPS, e.g. seamless precise navigation going from outdoors to indoors. However, one must first make sure that UWB does not jam GPS! [11]

Acknowledgements

The Department of Transportation sponsored this research. In particular, great thanks go to Sally Frodge for her support.

We would like to thank Ming Luo and Dennis Akos for their help in this study. Finally, we'd like to thank the rest of the hard-working crowd at the Stanford GPS Laboratory for their help and support.

References

1. J.H. Williams, R.J. Davis, E.N. Rosario **Multipath Mitigation Performance of Planar GPS Adaptive Antenna Arrays for Precision Landing Ground Stations,** Institute of Navigation's GPS conference 2000
2. A.J. Van Dierendonck, Pat Fenton, and Tom Ford **Theory And Performance Of Narrow Correlator Spacing In A GPS Receiver**, Navigation, Fall 1992, Vol. 39, No. 3
3. Ross G. F. **The transient analysis of certain TEM mode 4-post networks** IEEE Transaction on Microwave Theory Tech. vol MTT-14, p 528, Nov 1966.
4. **Transmission and Reception System for Generating and Receiving Base-band Duration Pulse Signals without Distortion for Short Base-band Pulse Communication System,** U.S. Patent No. 3,728,632, 17 April 1973
5. Scheers, B.; Acheroy, M.; Vorst, A. Vander **Time domain modeling of UWB GPR and its application on landmine detection** Proceedings of SPIE, 2000
6. Kapoor, R.; Banerjee, A.; Tsihrintzis, G. A.; Nandhakumar, N. **UWB radar detection of targets in foliage using alpha-stable clutter models** IEEE Transactions on Image Processing, 1999
7. OSD/DARPA **Ultra-Wideband Radar review panel Assessment of Ultra-Wideband (UWB) technology** DARPA Arlington, VA, 1990
8. Yung-Fang Chen and M.D. Zoltowski, **Blind 2-D RAKE Receivers Based on RLS-Type Space-Time Adaptive Filtering for DS-CDMA System**,

Proceedings of the 1998 IEEE International Conference on Acoustics, Speech, and Signal Processing , Seattle, WA, May 12-15, 1998

9. Jeffrey H. Reed, Theodore S. Rappaport, Brian D.Woerner **Wireless personal communications** Kluwer Academic Publishers, 1996.
10. Win M. Z. and Scholtz R. A. **On the Robustness of Ultra-Wide Bandwidth Signals in Dense Multipath Environments** IEEE Communications Letters, Vol. 2, No. 2, 1998
11. Luo, M., Akos, D., Pullen, S., and Enge, P. **Interference to GPS from UWB transmitters.** Institute of Navigation's GPS conference, 2000